

# Generation and evolution of bright-dark pulses in a thulium/holmium co-doped fiber laser based on nonlinear polarization rotation\*

WANG Xiaofa\*\*, HE Yiping, and PAN Jiamin

Chongqing Key Laboratory of Photoelectronic Information Sensing and Transmitting Technology, School of Optoelectronic Engineering, Chongqing University of Posts and Telecommunications, Chongqing 400065, China

(Received 28 November 2022; Revised 4 June 2023)

©Tianjin University of Technology 2023

We report an experimental phenomenon of the splitting and merging of the bright-dark pulses (BDPs) in a mode-locked thulium/holmium co-doped fiber laser (THDFL) based on nonlinear polarization rotation (NPR). By adding 100-m-long highly nonlinear fiber (HNLF) into a simple ring cavity, the BDPs can be generated. The time interval between the bright and dark pulses increases linearly with the pump power and approximately equals to the inverse of the modulation frequency of the radio frequency (RF) spectrum. Apart from that, the bright and dark pulses are shown not to be orthogonally polarized. The obtained results are valuable for the evolutionary mechanism of the BDPs in passively mode-locked fiber lasers (PMLFLs).

**Document code:** A **Article ID:** 1673-1905(2023)12-0710-6

**DOI** <https://doi.org/10.1007/s11801-023-2200-4>

To date, various types of pulses have been experimentally obtained in passively mode-locked fiber lasers (PMLFLs), such as conventional solitons<sup>[1]</sup>, noise-like pulses<sup>[2]</sup>, higher-order solitons<sup>[3]</sup> and dissipative solitons<sup>[4]</sup>. In contrast to the bright pulses described above, there is the other type of pulse, the dark pulse, which has an intensity dip in the continuous wave (CW) background. The dark pulses have some advantages with low transmission loss in fiber, better stability in case of noise and being less affected by intra-pulse stimulated Raman scattering<sup>[5]</sup>. So the dark pulses have great potential applications in optical communication systems. According to the interaction of solitons, there are some pulse pairs including bright-bright, dark-dark and bright-dark pulse (BDP) pairs in optical fiber systems. The pulse pairs have been studied theoretically by means of the nonlinear Schrödinger equation (NLSE)<sup>[6]</sup>. Within these pulse pairs, in addition to the great value of the BDPs in secure communication systems, they also have a wide range of potential applications in spectroscopy, optical communications and soliton evolution. So far, the BDPs have been implemented with different saturable absorbers (SAs) in PMLFLs. At present, SAs can be divided into real SAs and artificial SAs. Compared with real SAs, artificial SAs have the advantages of high damage threshold, high integration<sup>[7]</sup>, and they have been widely used in PMLFLs in 1–2  $\mu\text{m}$  band<sup>[8-12]</sup>. Among artificial SAs, nonlinear polarization rotation (NPR) is an effective

mechanism due to its higher damage threshold and shorter recovery time<sup>[13-16]</sup>. In 2016, LÜ et al<sup>[17]</sup> demonstrated an experimental study of the BDPs in ytterbium-doped fiber laser (YDFL) based on NPR. In 2018, WU et al<sup>[18]</sup> reported the generation and evolution of the dark-bright pulses and the conversion between the dark and bright pulses in an NPR-based erbium-doped fiber laser (EDFL). In 2019, WU et al<sup>[19]</sup> reported a dual-wavelength bright-dark soliton pair EDFL based on NPR. In 2020, WANG et al<sup>[20]</sup> reported the generation of the BDPs in a mode-locked thulium-doped fiber laser (TDFL) by employing the mode-locking technology of the NPR and nonlinear optical loop mirror (NOLM).

Apparently, the above literatures have focused on the generation of the BDPs and few literatures have studied the interaction of the BDPs under specific conditions. Furthermore, compared with the ytterbium-doped gain fiber and erbium-doped gain fiber, the thulium/holmium co-doped gain fiber has a wider emission spectrum with more pronounced mode competition effects, which may provide more possibilities for the interaction between the pulses. Thus, it's important to study the generation and evolution of the BDPs in NPR-based PMLFLs in 2  $\mu\text{m}$  band.

In this paper, the split and merge of the BDPs are investigated in a mode-locked thulium/holmium co-doped fiber laser (THDFL) by using the NPR technology. The BDPs can be realized by inserting 100-m-long highly

\* This work has been supported by the National Natural Science Foundation of China (No.6170031626), and the Natural Science Foundation of Chongqing City, China (Nos.cstc2018jcyjAX0585 and cstc2017zdxX0011).

\*\* E-mail: wangxf@cqupt.edu.cn

nonlinear fiber (HNLF) to the ring cavity. The time interval between the bright and dark pulses increases linearly with the pump power and presumably equals to the inverse of the modulation frequency of the radio frequency (RF) spectrum. Moreover, the bright and dark pulses aren't orthogonally polarized.

The experimental setup is shown in Fig.1. A 1 550 nm laser diode (LD) with the maximum output power of 1 W is used to provide the pump energy and a 1 550/1 950 nm wavelength division multiplexer (WDM) is employed to deliver the pump energy into the ring cavity. A 2.5 m section of thulium/holmium co-doped fiber (THDF, Coractive TH512) with a core/inner cladding diameter of 9/125  $\mu\text{m}$  has a core absorption of 13.3 dB/m at 1 550 nm and a dispersion parameter of  $-0.056 \text{ ps}^2/\text{m}$ . There are two polarization controllers (PC1, PC2) and a polarization-dependent isolator (PD-ISO) to form the NPR. The cavity is added to  $\sim 100\text{-m}$ -long HNLF (nonlinear coefficient of  $\sim 10 \text{ W}^{-1} \cdot \text{km}^{-1}$ ), which is the key component for generating the BDPs. To output the laser signal, an output coupler (OC) with a splitting ratio of 30% is introduced. The rest of the fibers in the cavity are single-mode fibers (SMF28e) with a dispersion parameter of  $-0.071 \text{ ps}^2/\text{m}$ . The total cavity length is  $\sim 119.46 \text{ m}$  and the net cavity dispersion is estimated as  $-1.344 \text{ ps}^2/\text{m}$ . Outside the cavity, a polarizing beam splitter (PBS) and a three-paddle PC3 are applied to study the polarization characteristics of the BDPs. In the experiment, the output characteristics of the THDFL are monitored by an optical spectrum analyzer (Omni- $\lambda$  750i, Zolix) with a resolution of 0.05 nm, a 1 GHz oscilloscope (WaveRunner 610Zi, Lecroy) and an RF spectrum analyzer (FSL3, Rohde & Schwarz) with 3 GHz bandwidth. In addition, both the oscilloscope and the RF spectrum analyzer should be worked together with an InGaAs photodetector (ET-5000F, EOT).

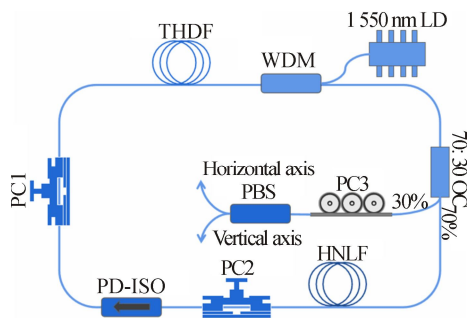


**Fig.1 Experimental setup of the THDFL**

The relationship between the average output power of the THDFL and the pump power is firstly studied. As shown in Fig.2, the average output power increases approximately linearly as the pump power increases. The oscillation threshold of the THDFL is 0.4 W and the slope efficiency can be calculated to be  $\sim 8.63\%$ . The high threshold and low slope efficiency are caused

mainly by the mode field mismatch between the THDF and the pigtail of WDM, and the large loss of HNLF in 2  $\mu\text{m}$  band. When the pump power reaches the oscillation threshold, the THDFL operates in four regimes including CW (0.4—0.45 W), basic mode-locking (BML, 0.45—0.5 W), transition regime (TR, 0.5—0.55 W) and BDP (0.55—1 W).

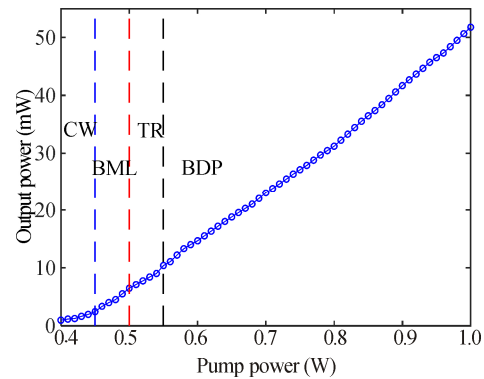


**Fig.2 Average output power under different pump powers**

In our experiment, when the pump power exceeds 0.45 W, the BML pulses are obtained by adjusting PC1 and PC2 carefully. Fig.3 presents the laser output performance with a pump power of 0.5 W. In Fig.3(a), the interval between adjacent pulses is 0.58  $\mu\text{s}$ , corresponding to the fundamental repetition frequency of  $\sim 1.72 \text{ MHz}$ , which match with the cavity length. The inset of Fig.3(a) shows the single BML pulse and there is a pair of pulses with small amplitude on its right side. Fig.3(b) displays the corresponding optical spectrum. The central wavelength and full width at half maximum (*FWHM*) are 1 912.40 nm and 6.34 nm, respectively. From Fig.3(b), we can see that there existed no Kelly sideband in the optical spectrum, which may be due to the spectral filtering effect caused by the birefringence property of the SMF in the cavity and the PCs together<sup>[19,21]</sup>. But there are some dips which are induced by the absorption of 2  $\mu\text{m}$  band laser by water molecules and carbon dioxide. The corresponding RF spectrum with a resolution bandwidth (*RBW*) of 1 kHz and a wide span of 200 MHz is depicted in Fig.3(c). Clearly, it shows a good stability of the BML pulse. Besides, the RF spectrum is flat and there is no modulation phenomenon. Fig.3(d) shows the fitting autocorrelation trace of the BML pulses.

Next, when the pump power is between 0.5 W and 0.55 W, the laser works in TR. In this regime, the BML pulses are unstable, which may be caused by environmental perturbations and soliton interactions<sup>[22]</sup>. Once we continue to adjust PC1 and PC2 properly, the stable BDPs are obtained. The generation of the BDPs may be mainly attributed to the high nonlinear effect of the HNLF<sup>[18,19]</sup>. Fixing PC1 and PC2, we gradually increase the pump power from 0.55 W to 1 W in steps of 0.05 W.

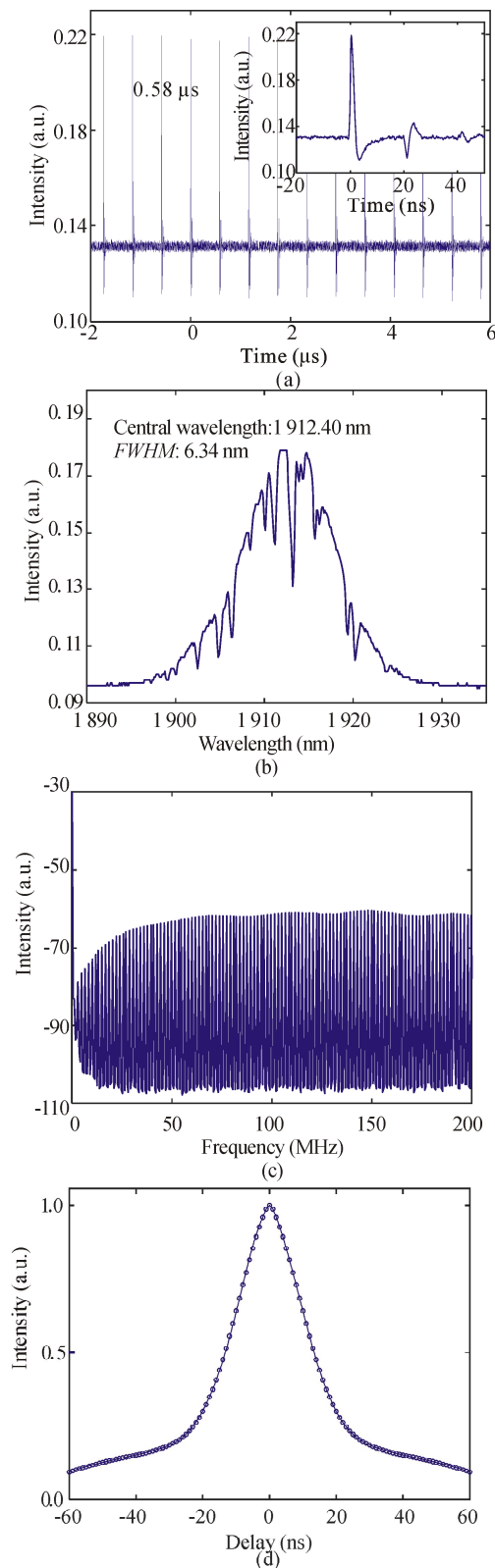


**Fig.3 Output characteristics of the BML pulses: (a) Typical pulse trains (inset: single pulse); (b) Optical spectrum; (c) RF spectrum; (d) Autocorrelation trace**

During this process, it is easy to observe that the split and merge of the BDPs are simultaneously generated. The evolutionary laws of the BDPs at the fundamental

repetition frequency are recorded when the pump power rises from 0.6 W to 1 W, as shown in Fig.4. In Fig.4(a), as the pump power increases, the high-intensity dark pulse (red dotted line) moves away from the high-intensity bright pulse and merges with the low-intensity dark pulse (blue dotted line) into a dark pulse of larger amplitude. Meanwhile, the high-intensity bright pulse remains constant while the low-intensity bright pulse keeps moving to the right. Subsequently, we reduce the pump power and find an interesting phenomenon of the reverse evolution of the BDPs. Therefore, we infer that the origin of the split and merge of the BDPs can be attributed to the higher laser gain caused by the increased emitted pump power, which may interfere with the balance between the parameters of laser<sup>[23]</sup>. Further speaking, under certain conditions, there is a clear interaction (split, merge, etc.) between them when the bright and dark pulses have a very small interval in the time domain<sup>[24]</sup>. In addition, we guess that the large amplitude dark pulses generated will split if the pump power continues to be increased<sup>[23-25]</sup>. The similar evolutionary phenomenon of the BDPs can also be realized when we adjust the intracavity PCs. The split of the BDPs has a clear evolutionary feature in that the time interval between the bright and dark pulses increases presumably linearly with the increasing pump power. Fig.4(b) plots the corresponding optical spectrum. As the pump power increases, the spectral intensity obviously increases while the central wavelength and *FWHM* don't change significantly. Fig.4(c) shows the corresponding RF spectra with an *RBW* of 1 kHz and a wide span of 300 MHz with different pump powers. It is clear to see that the RF spectra have a distinct modulation phenomenon, which is similar to Ref.[26]. The modulation frequency decreases from 218.5 MHz to 49.9 MHz when the pump power increases from 0.6 W to 1 W. After calculation, we know that the modulation frequency is approximately equivalent to the reciprocal of the time interval between the bright and dark pulses. As Fig.4(d) shows, a linear relation between the inverse of the modulation frequency and the pump power is observed.

Then, we focus on the output characteristics of the BDPs at the pump power of 1 W, as shown in Fig.5. Fig.5(a) plots the pulse trains of the BDPs. The interval of adjacent pulses is still 0.58 μs. The single pulse is given in the inset of Fig.5(a). It can be seen that the shapes and amplitudes of the bright and dark pulses are slightly different and there is a bright pulse with low-intensity to the right of the dark pulse, which is similar to the case in Ref.[27]. Fig.5(b) presents the corresponding optical spectrum. Its central wavelength locates at 1934.50 nm and the *FWHM* is 10.23 nm. The corresponding RF spectrum is measured, as shown in Fig.5(c). The signal-to-noise ratio (*SNR*) of ~40 dB indicates the good stability of the BDPs. The wide span of the RF spectrum is also shown in the inset of Fig.5(c). Fig.5(d) presents the fitting autocorrelation trace of the BDPs.

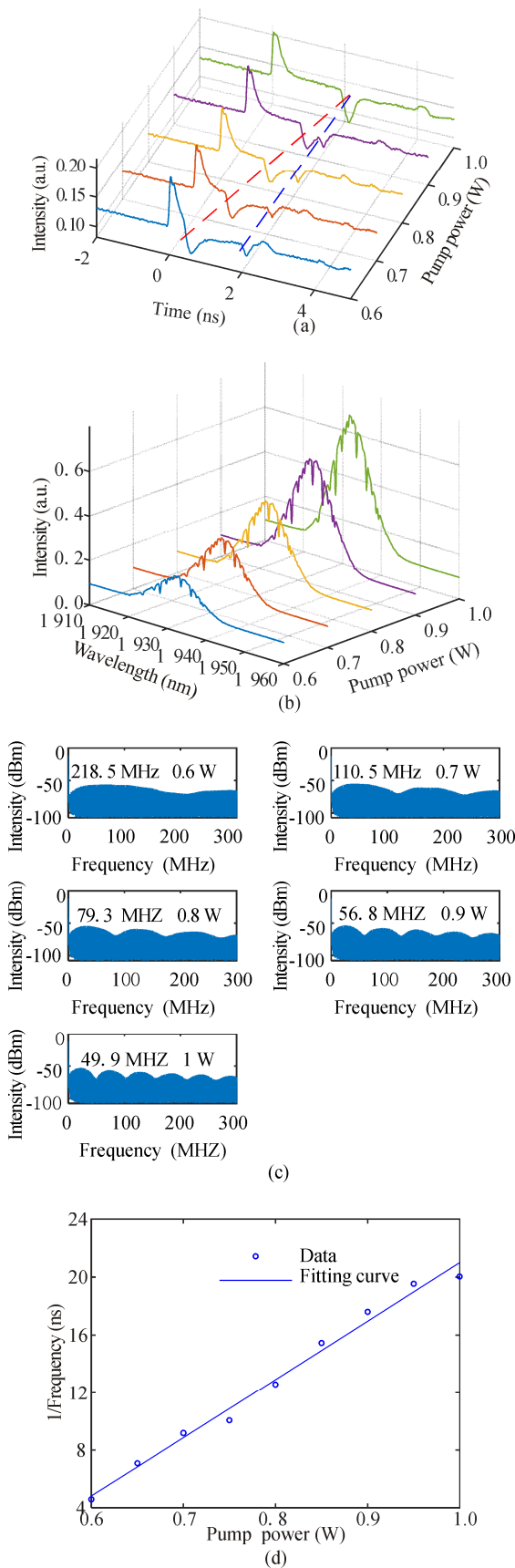


**Fig.4** Evolution characteristics of the BDPs: (a) Single pulses; (b) Optical spectra; (c) RF spectra; (d) Variation of the inverse of the modulation frequency

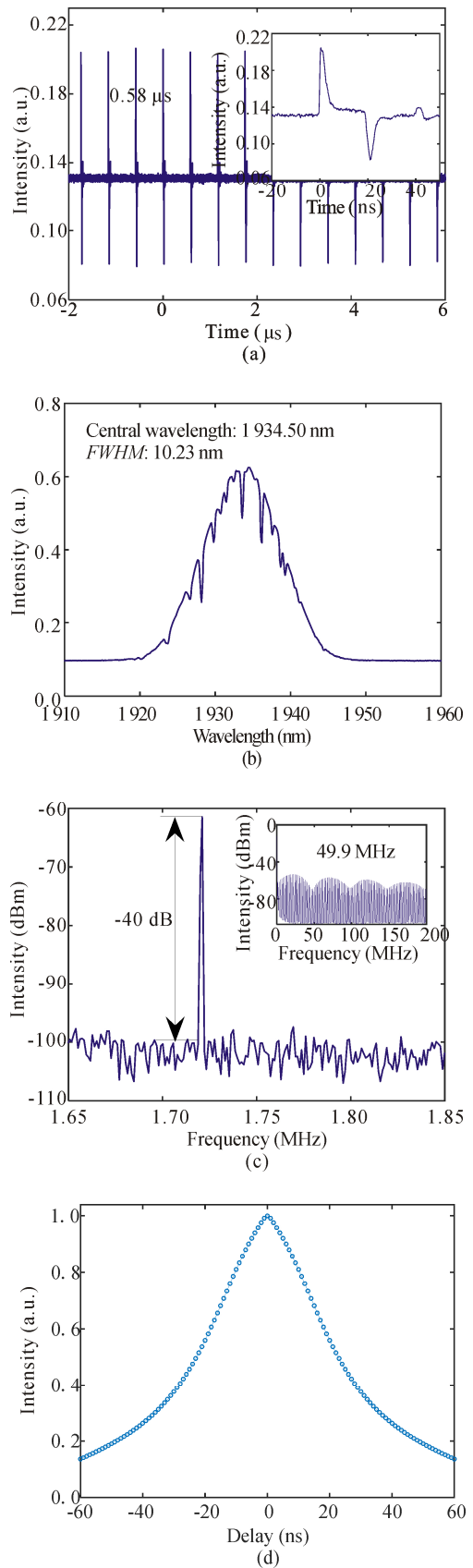


**Fig.5** Output characteristics of the BDPs: (a) Typical pulse trains (inset: single pulse); (b) Optical spectrum; (c) RF spectrum (inset: wide span of 200 MHz); (d) Autocorrelation trace

Finally, in order to study the polarization characteristics of the BDPs, the external cavity combiner of PC3 and PBS is used to monitor the two orthogonal polarization components. Regardless of how the PC3 is adjusted, the bright and dark pulses are observed simultaneously in both the horizontal and vertical axes of the PBS, which is similar to Refs.[28] and [29]. Fig.6 shows the temporal waveforms and the spectra measured without and with passing through PBS. From Fig.6(a), we can easily see that the two pulse polarization components have a uniform pulse sequence and the only difference is the amplitude disagreement compared to the pulses without passing PBS. As in the case of the time domain, Fig.6(b) displays the corresponding optical spectra of the two pulse polarization components, which differ mainly in magnitude. In addition, the characteristics of the RF spectrum remain unchanged. Therefore, we can draw the following conclusion. The bright and dark pulses are linearly polarized light that doesn't possess an orthogonal electric vector vibration direction. That is, in our experiments, the polarization state of the bright pulse and dark pulse is the same, which can coexist in any polarization.

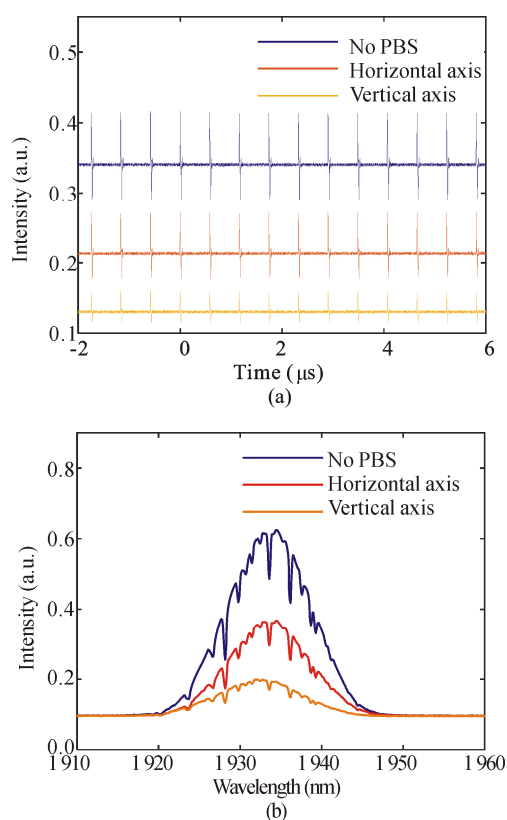


**Fig.6 Polarization characteristics of the BDPs: (a) Oscilloscope traces; (b) Optical spectra**

In conclusion, we have reported the split and merge of the BDPs in an NPR-based THDFL. By increasing the pumping power from 0.55 W to 1 W, it is easy to notice that the high-intensity dark pulse gradually moves away from the high-intensity bright pulse and merges with the low-intensity dark pulse to a larger dark pulse. We also

find that the same evolutionary law can be observed by adjusting PCs. What's more, the RF spectrum of the BDPs has a remarkable envelope modulation phenomenon in our work. In the end, using the PC and PBS to determine the polarization characteristics of the BDPs, we observe that the bright and dark pulses can't be separated, which means that the bright and dark pulses aren't orthogonally polarized. We believe that these results are useful for the theoretical and experimental studies on the evolution of the BDPs in PMLFLs.

### Ethics declarations

### Conflicts of interest

The authors declare no conflict of interest.

### References

- [1] WANG X F, ZHANG J H, PENG X L, et al. Generation and evolution of multiple operation states in passively mode-locked thulium-doped fiber laser by using a graphene-covered-microfiber[J]. *Chinese physics B*, 2018, 27(8): 084215.
- [2] CHEN L F, WU Q C, YAO Y, et al. Wavelength-switchable noise-like square pulsed fiber laser based on nonlinear effects[J]. *Optical fiber technology*, 2022, 74: 103066.
- [3] XIE S Z, JIN L, ZHANG H, et al. All-fiber high-power spatiotemporal mode-locked laser based on multimode interference filtering[J]. *Optics express*, 2022, 30(2): 2909-2917.
- [4] HUANG S T, ZHENG S K, WANG J C, et al. Tunable mode-locked Tm-doped fiber laser based upon cross-phase modulation[J]. *Optics express*, 2022, 30(18): 32256-32266.
- [5] SONG Y F, SHI X J, WU C F, et al. Recent progress of study on optical solitons in fiber lasers[J]. *Applied physics reviews*, 2019, 6(2): 021313.
- [6] AFANASYEV V V, KIVSHAR Y S, KONOTOP V V, et al. Dynamics of coupled dark and bright optical solitons[J]. *Optics letters*, 1989, 14(15): 805-807.
- [7] WANG Z H, ZHANG B, LIU J, et al. Recent developments in mid-infrared fiber lasers: status and challenges[J]. *Optics and laser technology*, 2020, 132: 106497.
- [8] WANG F, ZHANG X L, CUI J H. Tm-doped fiber laser with multiwavelength output and switchable wavelength difference based on nonlinear polarization rotation effect[J]. *Optics and laser technology*, 2020, 130: 106343.
- [9] QIU H X, PAN Y Z, WANG X P, et al. Raman-enhanced multicolor pulses in dissipative soliton mode-locked ring-cavity fiber laser based on GIMF-SA[J]. *Optik*, 2022, 262: 169390.
- [10] WU C H, YAO Y, WU Q C, et al. Noise-like pulses under different intra-cavity nonlinearity[J]. *Optical fiber technology*, 2021, 64: 102549.
- [11] LI H J, LI X L, ZHANG S M, et al. Vector staircase

- noise-like pulses in an Er/Yb co-doped fiber laser[J]. *Journal of lightwave technology*, 2022, 40(13): 4391-4396.
- [12] WANG X, KOMAROV A, KLIMCZAK M, et al. Generation of noise-like pulses with 203 nm 3-dB bandwidth[J]. *Optics express*, 2019, 27(17): 24147-24153.
- [13] DONG Z P, LIN J Q, LI H X, et al. Er-doped mode-locked fiber lasers based on nonlinear polarization rotation and nonlinear multimode interference[J]. *Optics and laser technology*, 2020, 130: 106337.
- [14] PU G Q, ZHANG L, HU W S, et al. Automatic mode-locking fiber lasers: progress and perspectives[J]. *Science China information sciences*, 2020, 63(6): 1-24.
- [15] AHMAD H, AZMY N F, NORISHAM N F, et al. Thulium-doped fluoride mode-locked fiber laser based on nonlinear polarization rotation[J]. *Optical and quantum electronics*, 2022, 54(2): 1-11.
- [16] STEINBERG D, ZAPATA J D, SAITO L A M, et al. Study of pulse formation in an EDFL under a large dispersion variation hybridly mode-locked by graphene and nonlinear polarization rotation[J]. *IEEE photonics journal*, 2021, 13(2): 1-14.
- [17] LÜ Z G, TENG H, FANG S B, et al. A harmonically mode-locked dark soliton and bright-dark soliton pair ytterbium fiber laser[J]. *Journal of optics*, 2016, 18(6): 065502.
- [18] WU Q C, GU Y L, YAO Y, et al. Convertible dark pulse and bright pulse fiber ring laser by adjusting the polarization[J]. *IEEE photonics technology letters*, 2018, 30(14): 1285-1288.
- [19] WU Q C, YAO Y, YANG Y F, et al. Repetition rate adjustable dual-wavelength solitons fiber laser based on highly nonlinear fiber[C]//2019 Photonics & Electromagnetics Research Symposium-Spring (PIERS-Spring), June 17-20, 2019, Rome, Italy. Berlin, Heidelberg: Springer-Verlag, 2019: 2385-2390.
- [20] WANG X F, LIU D X, HAN H H, et al. Generation of cavity-birefringence-dependent multi-wavelength bright-dark pulse pair in a figure-eight thulium-doped fiber laser[J]. *Chinese physics B*, 2021, 30(5): 054205.
- [21] GUO B, YAO Y, YANG Y F, et al. Topological insulator: Bi<sub>2</sub>Se<sub>3</sub>/polyvinyl alcohol film-assisted multi-wavelength ultrafast erbium-doped fiber laser[J]. *Journal of applied physics*, 2015, 117(6): 063108.
- [22] LI H F, ZHANG S M, DU J, et al. Passively harmonic mode-locked fiber laser with controllable repetition rate based on a carbon nanotube saturable absorber[J]. *Optics communications*, 2012, 285(6): 1347-1351.
- [23] WANG X, ZHOU P, WANG X L, et al. 2 μm bright-dark pulses in Tm-doped fiber ring laser with net anomalous dispersion[J]. *Applied physics express*, 2014, 7(2): 022704.
- [24] WANG Y M, HUANG H, LI X H, et al. Controllable soliton pairs in few-layer FePSe<sub>3</sub> nanosheets-based optical-intensity modulators[J]. *ACS applied nano materials*, 2020, 3(8): 7713-7719.
- [25] YANG H R, LI X P, WANG Y, et al. TaSe<sub>2</sub>-based mode-locked fiber laser with four switchable operating states[J]. *Optics and laser technology*, 2021, 138: 106924.
- [26] WANG X F, WANG J, DUAN X Y. Experimental investigation on evolution of a split multi-wavelength bright-dark pulse in a mode-locked thulium-doped fiber laser[J]. *Optoelectronics letters*, 2022, 18(12): 0717-0722.
- [27] ZHAO J Q, YAN P G, RUAN S C. Observations of three types of pulses in an erbium-doped fiber laser by incorporating a graphene saturable absorber[J]. *Applied optics*, 2013, 52(35): 8465-8470.
- [28] MENG Y C, ZHANG S M, LI H F, et al. Bright-dark soliton pairs in a self-mode locking fiber laser[J]. *Optical engineering*, 2012, 51(6): 064302.
- [29] LI X L, ZHANG S M, MENG Y C, et al. Harmonic mode locking counterparts of dark pulse and dark-bright pulse pairs[J]. *Optics express*, 2013, 21(7): 8409-8416.